

# Aerodynamic Modeling of Folded Fin for Unfolding Motion Simulation

Suk Young Jung\*

Agency for Defense Development, Taejon 305-152, Republic of Korea  
and

Sung Joon Yoon†

LIG Nex1 Company, Ltd., Seoul 135-982, Republic of Korea

DOI: 10.2514/1.46735

**The dynamic motion of the folded fins of a missile during the launching phase is quite complex. A simulation of the unfolding fin motion requires a realistic model for applied loads acting on the folded fin. One of these important applied loads is the aerodynamic force exerting on the fin. In this study, the aerodynamic force was modeled and an efficient way to evaluate the aerodynamic damping moment was suggested; then the unfolding motion of the fin was simulated using the aerodynamic model. The simulation results, using the aerodynamic model including damping, agreed quite well with the test results. Although simple, the suggested aerodynamic modeling technique for the unfolding fin turned out to be efficient and reliable enough to provide data for the analysis of the unfolding mechanism for a missile system.**

## Nomenclature

$A$	=	moment due to aerodynamic force acting on fin, $N \cdot m$
$A_{ref}$	=	reference area for aerodynamic folding moment/ damping coefficient
$C$	=	static aerodynamic folding moment coefficient
$C_{\psi}$	=	aerodynamic damping coefficient
$F$	=	moment due to friction force acting around folding hinge of fin, $N \cdot m$
$G$	=	moment due to gravitational force exerting on fin, $N \cdot m$
$I_{XX}$	=	moment inertia of rotating part of folded fin about the axis of folding hinge, $kg \cdot m^2$
$K$	=	spring moment coefficient, $N \cdot m/deg$
$L_{ref}$	=	reference length for aerodynamic folding moment/ damping coefficient, $m$
$M$	=	mass of rotating part of the folded fin, $kg$
$q_{\infty}$	=	freestream dynamic pressure, $Pa$
$V_{\infty}$	=	freestream velocity, $m/s$
$Y_{C.G.}$	=	span length between the axis of folding hinge and center of mass of rotating part of fin, $m$
$Y_{TIP}$	=	span length between the axis of folding hinge and tip of fin, $m$
$Z$	=	spring torque, $N \cdot m$
$\alpha$	=	angle of attack
$\alpha_{TIP}$	=	induced angle of attack at fin tip due to rotating motion of unfolding fin
$\beta$	=	angle of sideslip
$\Psi$	=	folding angle, $deg$

## I. Introduction

**N**OWADAYS, many missiles are developed to be contained in a tube or canister for the convenience of storage, delivery, and loading on a launcher, which requires a mechanism to fold the fins when stored and to unfold them when in flight [1]. Figure 1 shows a missile just firing out of a launch tube, with some of its fins

completely deployed and others in the process of unfolding. Because fins produce aerodynamic force for stability and maneuverability during flight, the mechanism must guarantee the successful deployment of all the fins under any circumstances. For this purpose, an unfolding device could be contrived and designed to produce enough torque for the complete deployment of fins even under extreme operational conditions, such as a high blast of wind. Besides the torque generated by the unfolding device, some physical phenomena are related to the fin unfolding process regardless of whether they help or hamper it; thus, it is essential to consider the aerodynamic load exerting on the unfolding fins of an accelerating missile in a high-wind environment.

Kayser and Brown [2] analyzed the motion of hinged fins with an approximate model of the aerodynamic folding moment while neglecting the effect of gravity and hinge friction. In their model, the aerodynamic force acting on the fin was estimated by using an analogy with the rolling moment generated by the fin and as a function of fin deployment angle. The rolling moment on the fully deployed fin due to cant angle and the effective yawing angle were introduced to estimate the folding moment during fin deployment; they also considered the wind velocity vector variations according to the fin deployment motion. They used a relatively simple model for the aerodynamic folding moment, assuming a fixed position of the pressure center during fin deployment and using vector algebra to calculate the wind angle according to projectile and fin motion. McGrath [3] calculated the aerodynamic folding moment of the folded fins of the Tactical Tomahawk with VSAERO, a commercial panel method solver that effectively obtains the data on a large number of database points in a short time frame. Though the panel method, a lower-order computational tool, was applied to the flow analysis around a complex geometry, comparisons between the computations and wind-tunnel (WT) results showed good agreement, except in cases in which the folded fin was positioned close to the missile body. A comparison of the computation results of two different missile configurations with and without a booster showed that the booster attached to the missile base acts like a dam to increase the pressure of flow, thereby changing the flowfield around the fin attached to the boat-tail section of the missile close to the booster and lessening the adverse aerodynamic folding moment.

In addition to static aerodynamic load, dynamic effects of aerodynamic characteristics on the body should be included for the precise prediction of its motion. One way to handle the dynamic effect is to include the damping coefficients in the dynamic model. Theoretically and experimentally, characteristics and techniques of evaluation and measurement of the aerodynamic damping coefficient

Received 14 August 2009; revision received 7 January 2010; accepted for publication 24 January 2010. Copyright © 2010 by the American Institute of Aeronautics and Astronautics, Inc. All rights reserved. Copies of this paper may be made for personal or internal use, on condition that the copier pay the \$10.00 per-copy fee to the Copyright Clearance Center, Inc., 222 Rosewood Drive, Danvers, MA 01923; include the code 0022-4650/10 and \$10.00 in correspondence with the CCC.

\*Principal Researcher, Yuseong-gu. Member AIAA.

†Research Fellow, Precision Guided Munitions Laboratory. Senior Member AIAA.

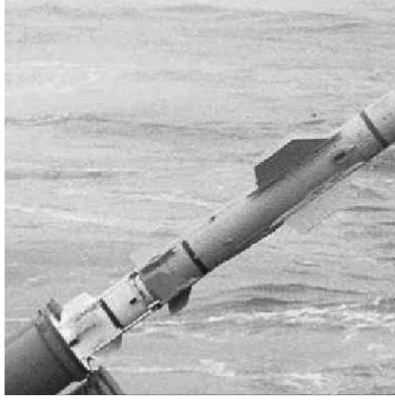


Fig. 1 Unfolding fins of a launching missile.

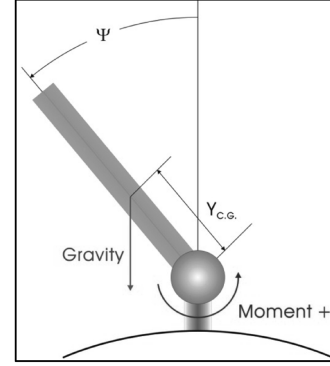


Fig. 2 Diagram of fin unfolding motion.

have been widely studied. Owing to recent achievements in high-performance computation technology, the aerodynamic damping coefficient can be obtained through unsteady computation with a 3-D geometry. But it is not an easy task to get the aerodynamic damping efficiently by numerical computations or even by experiments.

Kayser and Brown [2] pointed out that the effective angle of yaw was critical in determining the magnitude of the rolling moment, which was varied according to the angular rates of the projectile and its unfolding fin. They also made a relation between the effective angle of yaw and a cant angle based on the roll moment of a nonspinning projectile. Similar modeling for roll damping coefficients can be seen in an empirical correlation between the roll damping of a cruciform-tailed missile and the rate of roll moment due to the cant angle of the tail, as proposed by Eastman [4].

In this study, the aerodynamic folding moment coefficient was set to consist of two components: static and damping. The static aerodynamic loads were measured during the wind-tunnel test, and the damping coefficients were obtained from the numerical computations. The aerodynamic damping coefficients were computed at each point of flight condition by the commercial panel code ZONAIR. The geometry of the fin was twisted to take into account the flow angle change due to the rotating motion of the unfolding fin. The angles of the camber line along the fin span were varied according to the freestream and local velocities of the corresponding fin section. Based on the aerodynamic and other models of moment, the motions of the unfolding fin were analyzed and compared with the wind-tunnel-test results, which measured the performance of the unfolding mechanism. The results from the simulation including the aerodynamic damping model agreed well with the wind-tunnel-test results.

## II. Dynamics Model of Unfolding Fin

### A. Dynamics Model

Figure 2 shows the unfolding fin rotates about a folding hinge as a center of rotation, under the influence of moments such as torque generated by the unfolding device, for example, spring, and moments due to various physical phenomena, such as aerodynamic, gravitational, and frictional forces, etc. The equation governing the motion of unfolding fin is given under the assumption of no movement of the folding hinge or relative motion to the missile frame:

$$I_{XX} \ddot{\Psi} = Z + G + F + A \quad (1)$$

The axis of rotation, coincident with the axis of the folding hinge, is assumed to be perfectly aligned with the missile axis so that no coupling term appears in the equation. The right-hand side of the equation contains external moments acting on the folded fin. Spring torque,  $Z$ , can be formulated as a linear function of the folding angle with the initial torque,  $Z_0$ , when the fin is fully folded, where  $\Psi = \Psi_0$ :

$$Z(\Psi) = Z_0 + K(\Psi - \Psi_0) \quad (2)$$

The moment by gravitational force,  $G$ , can be also described as follows:

$$G(\Psi) = MgY_{C.G.} \sin \Psi \quad (3)$$

The moment due to friction between the hinge and rotating parts of the fin,  $F$ , is set to be constant in this study. This value can be obtained by comparing the simulation results without aerodynamic effects to the unfolding device performance tests conducted in the ground.

### B. Aerodynamic Folding Moment

Aerodynamic force plays a critical role in the behavior of unfolding fin. Under aerodynamically severe conditions, the aerodynamic fin-folding moment grows enough to hamper the unfolding process. Thus, the accurate prediction of the aerodynamic moment is a key element in the simulation of the fin unfolding motion and the design of the unfolding device.

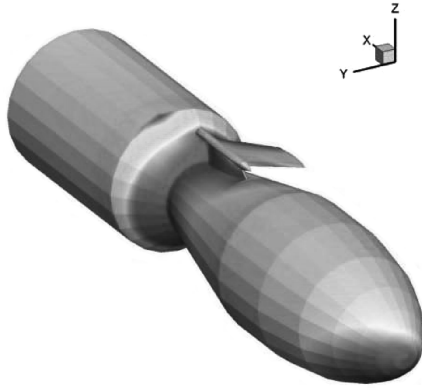
The aerodynamic fin-folding moment is assumed to consist of a static aerodynamic folding moment and aerodynamic damping moments that resist angular motion of the fin:

$$A(\alpha, \beta, q_\infty, \Psi, \dot{\Psi}) = [C(\alpha, \beta, \Psi) + C_{\dot{\Psi}}(\alpha, \beta, \Psi)\dot{\Psi}]q_\infty A_{ref} L_{ref} \quad (4)$$

Each term of the aerodynamic folding moment is defined by using a static aerodynamic fin-folding moment coefficient and a damping coefficient, respectively. Whereas the aerodynamic damping moment is assumed to be proportional to the angular speed, the damping coefficient is set to be independent of the angular speed as usual. Both coefficients are varied according to the aerodynamic conditions, the angle of attack and sideslip, and the folding angle.

Each aerodynamic coefficient can be obtained in various ways, such as a wind-tunnel test or a calculation using theoretical and numerical methods. For the purpose of this study, tests were conducted in subsonic wind tunnel at the Agency for Defense Development in the Republic of Korea, using a test model with the same configuration as shown in Fig. 3. The geometry of the model, the folding angle, was fixed during the test and a balance was installed inside the model to measure the force acting on the folded part of the fin, which is isolated from the folding hinge and the root section supporting the folding hinge.

Applying a modern 3-D turbulent flow solver, however, requires enormous effort and time to build a computational grid system around the complex geometry of a missile body and folded fins with various folding angles and to fulfill the large number of data points needed to cover the various flight and operational conditions. Figure 3 shows a panel system of the test model with a fin folded up to 112.5 deg attached to its back. Surface pressures on the model are also shown, and these steady-state results were computed using the panel method with the aerodynamic conditions described in the figure. The model took the shape of a shortened missile with a booster attached at its base and located just behind the folded fin. The model was tested with a booster because the booster might influence the flow around the tail fins [3]. Fins folded at various folding angles to missile body are shown in Fig. 4, and computations were carried out using the panel system for those configurations. Figure 5 compares



$M_{\infty}=0.2, \alpha=10 \text{ deg}, \beta=10 \text{ deg}, \Psi=112.5 \text{ deg}$

Fig. 3 Panel for wind-tunnel test model and pressure distribution.

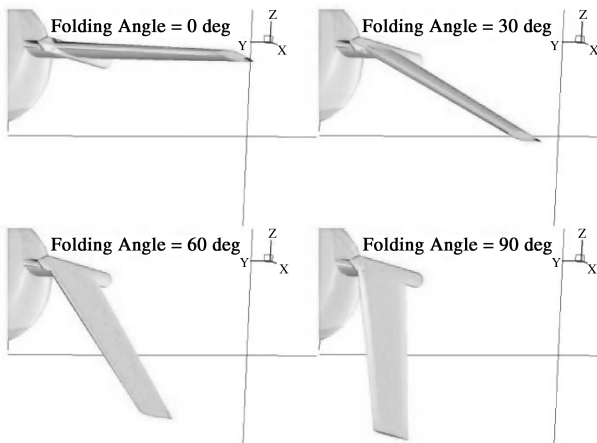


Fig. 4 Configuration of fin folded to various angles.

the static aerodynamic coefficients obtained from the wind-tunnel test and the numerical computation of the panel method, which has, over modern computational fluid dynamics (CFD) schemes, the advantage of efficient computation, including buildup of the panel only on the surface and not in space, and the disadvantage of inaccurate results, especially when the viscous effect appears significantly. As the folding angle increases, the fin gets closer to missile body and more interference occurs between the flow and the close walls of the missile body and fin. The difference between the two coefficients shown in Fig. 5 may come from the shortcoming of the panel method. A similar tendency of discrepancies between the wind-tunnel-test and panel method results can be seen in [3].

During the numerical simulation using ZONAIR, no special treatment was adopted for the wake, which was originally set to emanate directly from trailing edge of the folding fin, and no separation between the fin surface and the missile body was considered. Studying the precise estimation of the aerodynamic characteristics seemed redundant because measured data were already available for this study. In Fig. 3, strong interactions between the wake and booster are shown to change the pressure field on the forehead of the booster but supposedly cause little effect on the fin itself.

### III. Aerodynamic Damping Model

#### A. Induced Angle of Attack

Dynamic effects, due to the rotating motion of the unfolding fin about the folding hinge axis, can be introduced using an aerodynamic damping coefficient that is defined as the rate change of the static aerodynamic folding moment coefficient due to a change in the angular velocity of the unfolding fin. It is possible to evaluate the

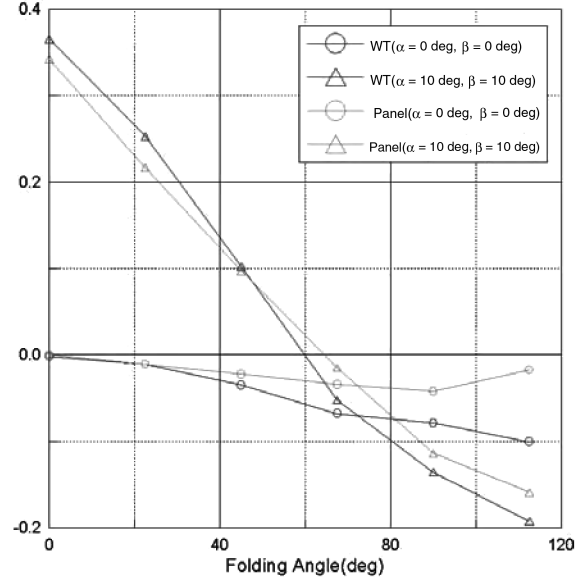


Fig. 5 Static aerodynamic folding moment acting on folded fin (comparison of measurement and computation).

damping coefficient using a wind-tunnel test or with a modern, high-fidelity CFD tool, which needs huge resources and consumes a lot of time to conduct a large number of tests and computations for the fulfillment of required database points. However, Etkin [5] showed how the linearized wing theory can be applied to estimate the longitudinal derivatives due to pitch rate on the wing by modifying a camber line as a curve according to the local angle of attack as calculated from the wind velocity and angular velocity along the cord of the wing.

The same technique can be applied to estimate the aerodynamic damping coefficient of the unfolding fin in a rotating motion. As seen in Fig. 6, the rotation of an unfolding fin creates an additional velocity component, normal to fin span axis and linearly distributed along the span. The velocity distribution can be represented by an additional velocity component at the fin tip,  $V_{TIP}$ , and the corresponding induced angle of attack at the fin tip,  $\alpha_{TIP}$ . The change in the aerodynamic characteristics of the fin can be described by using  $\alpha_{TIP}$ , with which the aerodynamic damping coefficient is defined:

$$C_{\dot{\Psi}} = \frac{\partial C}{\partial \dot{\Psi}} = \frac{\partial C}{\partial \alpha_{TIP}} \frac{\partial \alpha_{TIP}}{\partial \dot{\Psi}}; \quad \tan \alpha_{TIP} = \frac{V_{TIP}}{V_{\infty}} = \frac{Y_{TIP} \times \dot{\Psi}}{V_{\infty}} \quad (5)$$

By computing  $\frac{\partial C}{\partial \alpha_{TIP}}$ , the rate of change of the folding moment coefficient due to the induced angle of attack at the tip, an evaluation of the damping coefficient can be accomplished.

Additional velocity components due to the rotation motion can be directly imposed on the panel computation as part of the wall boundary condition [6]. Unfortunately, ZONAIR has no input option to include the rotational effect of the unfolding fin. To overcome this limit, the geometry of the fin was modified with twist along the span. The amount of twist was determined by the induced angle of attack, adopting a linear distribution of the induced angle of attack at the tip,  $\alpha_{TIP}$ , and 0 deg at the root. Figure 7 shows the fins twisted according to various  $\alpha_{TIP}$ ; those angles of camber line are varied linearly along

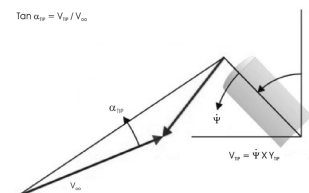


Fig. 6 Induced angle of attack due to rotation motion of unfolding fin.

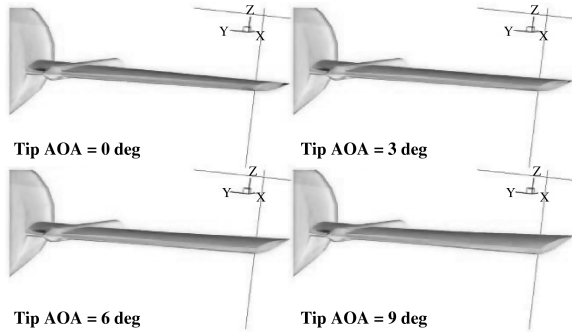


Fig. 7 Twisted fin configurations with various tip-induced angles of attack (AOA) when fully deployed.

span. Once static aerodynamic folding moments acting on an original fin ( $\alpha_{TIP} = 0$  deg) and a twisted one are computed, the derivative can be determined with a small  $\alpha_{TIP}$ :

$$\frac{\partial C}{\partial \alpha_{TIP}} \approx \frac{\Delta C}{\Delta \alpha_{TIP}} = \frac{C_{\alpha_{TIP}} - C_{\alpha_{TIP}=0 \text{ deg}}}{\alpha_{TIP}} \quad (6)$$

### B. Roll Damping of Wing-Alone Configuration

For validation, the technique was applied to evaluate the aerodynamic roll damping of the wing-alone configuration shown in Fig. 8 and compared with results using intrinsic functions in ZONAIR, which computes the aerodynamic damping coefficients, in other words, the aerodynamic stability coefficients, by calculating the difference of the aerodynamic coefficient due to a presumably small change in aerodynamic conditions with no change in geometry.

No intrinsic function of ZONAIR is applicable to the evaluation of the aerodynamic damping of the unfolding fin, and so the technique proposed to compute the damping coefficient uses ZONAIR as a flow solver to acquire the aerodynamic moment of a twisted fin.

A comparison of the roll damping coefficients from the two methods is shown in Fig. 8. One is obtained by using Eqs. (5) and (6) with the roll moment coefficients from the ZONAIR computations with a twisted fin but no change in flow condition. The other is from the ZONAIR computations with a small change of roll rate but the shape of the wing preserved. The good agreement between two methods shown in Fig. 8 imply the validity and feasibility of the current method.

## IV. Simulation of Deployment Motion of Folded Fin

### A. Fin Deployment Test

To measure the motion of the unfolding fin under aerodynamic load, fin deployment tests were performed with the model in Fig. 3 and in the same wind-tunnel facility. During the fin deployment test, a fin was initially set to be folded and tied; then the unfolding device was activated to start the unfolding motion after the wind speed inside the tunnel reached a desired level.

Table 1 Wind-tunnel-test conditions and results

Test no.	Wind speed, m/s	Angle of attack, deg	Sideslip angle, deg	Measured time for deployment, s
1	50	2	-6	0.190
2	60	3	-6	0.186
3	39	17	-32	X
4	40	17	38	0.108
5	35	14	-20	X
6	38	14	30	0.117
7	30	13	-11	0.163
8	32	13	-20	0.225
9	34	13	-28	X
10	35	17	-33	X
11	30	16	-37	0.160
12	34	0	-37	X

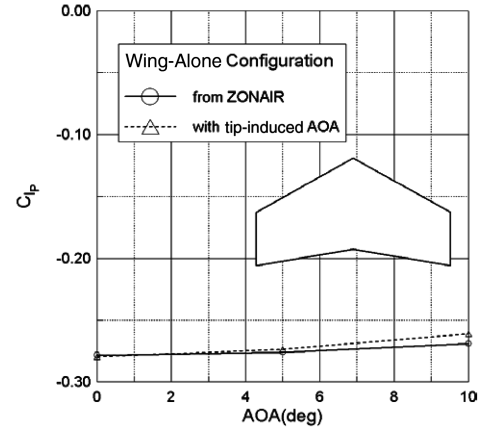


Fig. 8 Roll damping coefficient,  $C_p$  for wing-alone configuration.

The test conditions, listed in Table 1, can be divided into two groups. One is the high-speed low-angle case, which corresponds to the activation of the unfolding device after the missile gets more aligned to the wind to decrease angles of attack and sideslip while the missile gets more speed due to longer acceleration. The other is the low-speed high-angle case, which represents early activation so that high angles are imposed due to wind but the missile speed is relatively low. Test conditions were determined based on the results of the operational performance analysis of the missile system.

The time for fin unfolding in Table 1 was measured by counting the frames of image taken by high-speed cameras. In some tests, the fin failed to deploy fully, which is denoted in the table as an "X" instead of time. In determining the time from start to finish of the fin unfolding motion, a maximum error of two thousandths of a second can be used, because a resolution of 1000 frames per second was used during the fin deployment tests. Although the high-speed camera was used, folding angles were not measured.

### B. Simulation of Fin Unfolding Motion

Based on the governing equation and the dynamic models described in Eqs. (1–4), a simulation program was developed and applied to reproduce the results of the fin deployment tests shown in Table 1. In 5 tests out of 12, the fin failed to unfold completely, and the simulation results in Table 2 show the failure of the fin unfolding in the same cases as the test. In other test cases of successful unfolding, the unfolding times calculated from the simulations were quite similar to those measured in the tests. The aerodynamic database for these simulations contains the aerodynamic damping coefficients computed using the proposed procedure, as well as the aerodynamic folding moment coefficients measured in the wind-

Table 2 Simulation results of fin unfolding motion

Test no.	Measured time for deployment, s	Computed time for deployment, s		
		Complete aerodynamic model	Aerodynamic damping excluded	
			$F_{ORG}$	$F_{MOD}$
1	0.190	0.1864	0.1528	0.1776
2	0.186	0.1847	0.1425	0.1620
3	X	X	O	X
4	0.108	0.1080	0.1022	0.1071
5	X	X	O	X
6	0.117	0.1135	0.1077	0.1135
7	0.163	0.1611	0.1503	0.1691
8	0.225	0.2144	0.1770	X
9	X	X	X	X
10	X	X	O	X
11	0.160	0.1589	0.1412	0.1605
12	X	X	X	X

tunnel test. A realistic aerodynamic model of an unfolded fin is essential to an accurate simulation of the fin unfolding motion. From this comparison, it can be concluded that the proposed procedure is useful for evaluating the aerodynamic damping coefficient for an unfolding fin and for building a complete aerodynamic model for the analysis of fin unfolding motion.

Simulations with and without aerodynamic damping were performed and compared with test results. Table 2 shows the results of the simulation without the aerodynamic damping; there are some discrepancies between the test and simulation. Fins in simulations were deployed successfully in three out of five cases in which the fins were unfolded incompletely in the wind tunnel. And all the unfolding times were shorter than in the tests and the simulation with the aerodynamic damping, so that the differences in time between the test and the simulation increased as the aerodynamic damping was excluded from the aerodynamic database. The resisting force exerting on the unfolding fin would be underestimated because of the exclusion of aerodynamic damping from the simulation, and the lack of resistance would lead to faster deployment of the fin.

To compensate for the absence of the damping moment, the magnitude of the frictional moment was increased. An approximately 50% increase in friction,  $F_{MOD}$ , was needed to get the same results from the simulation as from the wind-tunnel test of five cases of unfolding failure. It is simpler to modify the friction model, assumed to be constant in this study, than to evaluate aerodynamic damping with many computations using the panel method.

Figure 9 shows the computed fin motions with the test 1 condition. Initially, the fin was folded fully and, when the fin was unfolded completely, the deployment angle became 0 deg. All the models gave similar fin motions, and the fastest unfolding motion and highest angular velocity were obtained with the force model of the original friction without aerodynamic damping. Little differences in fin motion were seen with the complete aerodynamic model including damping and the modified friction without damping. Both models take damping effects into account. While friction remains constant, the damping moment varies according to the folding angle and the angular velocity, which made a difference in simulated fin motions.

Simulated fin motions with three force models are shown for test 5 in Fig. 10. Excluding damping reduced the resistance to fin motion and resulted in full deployment, as opposed to the test results marked as "O" in Table 2, not only the time advance shown in Fig. 9. Other models including damping effects displayed incomplete fin unfolding, consistent with the test results. The simulation results of test 7 in Fig. 11 were similar to the previous results. In the simulation with the modified friction model, the angular velocity decreased more rapidly in the latter portion of the unfolding process and the fin deployment angle did not reach 0 deg; in other words, the fin failed to unfold.

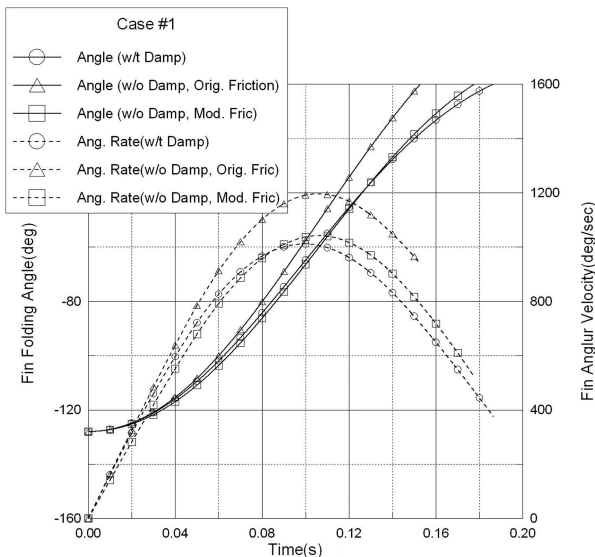


Fig. 9 Simulated fin motions with three force models (test 1).

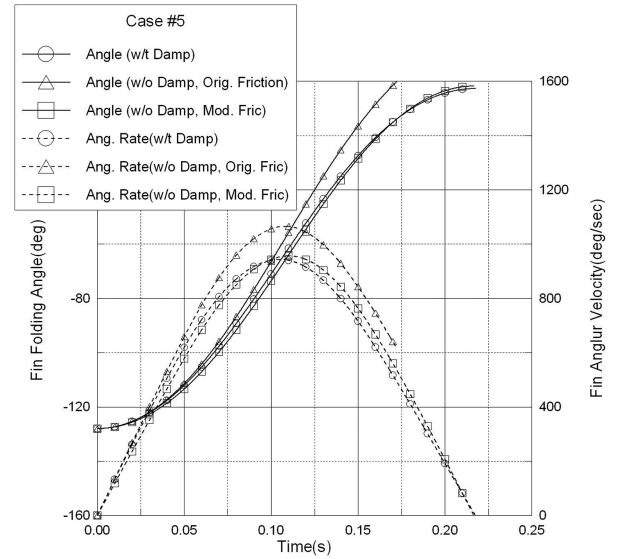


Fig. 10 Simulated fin motions with three force models (test 5).

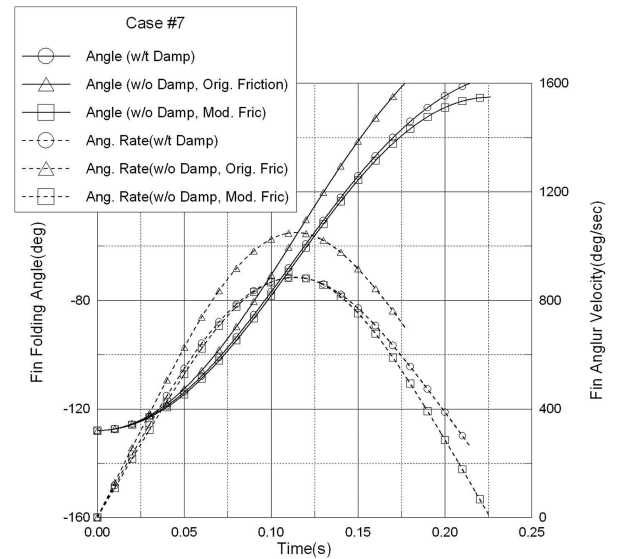


Fig. 11 Simulated fin motions with three force models (test 7).

The fin is considered to be in an unfolding motion while its angular velocity is positive. Once it drops below zero, the unfolding process stops and the fin fails to deploy. Thus, in the simulation, computation is ceased when the angular velocity of the fin decreases to zero. Modified friction appears to offer slightly more resistance to the fin unfolding motion, and a low value of angular velocity makes a critical difference in the success/failure of fin unfolding.

It can be concluded that the aerodynamic model including damping gave a more accurate database for the fin unfolding simulation and also reflected the mechanism of fin unfolding motion more precisely.

### V. Conclusions

For a fin unfolding motion analysis, the aerodynamic folding moment is assumed to consist of the static folding moment and the damping generated by the rotation motion of the fin around the folding hinge. Coefficients of the static folding moment and damping were obtained using a wind-tunnel test and computation using the panel method, respectively. To compute the damping coefficient, a technique was proposed to modify the geometries of the fin according to the rotation speed and to use the panel method as a

quasi-steady flow solver. Using the panel method, it was efficient to evaluate the damping coefficient and build the complete aerodynamic database.

Fin unfolding motions were simulated based on the aerodynamic database. The results compared quite well with the measurement done in the wind tunnel. If the aerodynamic damping moment was not included, the simulation results became less accurate.

### References

- [1] Kroyer, R., "Wing Mechanism Analysis," *Computers and Structures*, Vol. 72, 1999, pp. 253–265.  
doi:10.1016/S0045-7949(99)00044-9
- [2] Kayser, L. D., and Brown, T. G., "Fin Motion After Projectile Exit from Gun Tube," AIAA Paper 1992-4491, 1992.
- [3] McGrath, B. E., "Subsonic Aerodynamic Fin-Folding Moments for the Tactical Tomahawk Missile Configuration," AIAA Paper 2004-5193, 2004.
- [4] Eastman, D. W., "Roll Damping of Cruciform-Tailed Missiles," *Journal of Spacecraft and Rockets*, Vol. 23, No. 1, 1986, pp. 119–120.  
doi:10.2514/3.25794
- [5] Etkin, B., "Dynamics of Atmospheric Flight," Wiley, New York, 1972, pp. 267–273.
- [6] Lan, C. E., "A Quasi-Vortex-Lattice Method in Thin Wing Theory," *Journal of Aircraft*, Vol. 11, No. 9, Sept. 1974, pp. 518–527.  
doi:10.2514/3.60381

M. Miller  
Associate Editor